Review Article

Blood flow assessment technology in aortic surgery: a narrative review

Yu Hohri[1], Megan M. Chung[1], Viswajit Kandula[1], Ilya Kim[2], Jay Leb[3], Hideyuki Hayashi[1], Adham Elmously[1], Thomas FX O'Donnell[4], Virendra Patel[4], Vijay Vedula[5], Hiroo Takayama[1]

[1]Division of Cardiothoracic Surgery, Department of Surgery, New York-Presbyterian Hospital, Columbia University Medical Center, New York, NY, USA; [2]Department of Medicine, New York-Presbyterian Hospital, Weill Cornell Medical Center, New York, NY, USA; [3]Department of Radiology, New York-Presbyterian Hospital, Columbia University Medical Center, New York, NY, USA; [4]Division of Vascular Surgery, Department of Surgery, New York-Presbyterian Hospital, Columbia University Medical Center, New York, NY, USA; [5]Department of Mechanical Engineering, Columbia University in the City of New York, New York, NY, USA

Contributions: (I) Conception and design: Y Hohri, V Vedula, H Takayama; (II) Administrative support: V Vedula, H Takayama; (III) Provision of study materials or patients: Y Hohri, V Vedula; (IV) Collection and assembly of data: Y Hohri; (V) Data analysis and interpretation: Y Hohri, V Vedula, H Takayama; (VI) Manuscript writing: All authors; (VII) Final approval of manuscript: All authors.

Correspondence to: Hiroo Takayama, MD, PhD. Division of Cardiothoracic Surgery, Department of Surgery, New York-Presbyterian Hospital, Columbia University Medical Center, 707 Fort Washington Avenue, New York, NY 10032, USA. Email: ht2225@cumc.columbia.edu.

Background and Objective: Blood flow assessment is an emerging technique that allows for assessment of hemodynamics in the heart and blood vessels. Recent advances in cardiovascular imaging technologies have made it possible for this technique to be more accessible to clinicians and researchers. Blood flow assessment typically refers to two techniques: measurement-based flow visualization using echocardiography or four-dimensional flow magnetic resonance imaging (4D flow MRI), and computer-based flow simulation based on computational fluid dynamics modeling. Using these methods, blood flow patterns can be visualized and quantitative measurements of mechanical stress on the walls of the ventricles and blood vessels, most notably the aorta, can be made. Thus, blood flow assessment has been enhancing the understanding of cardiac and aortic diseases; however, its introduction to clinical practice has been negligible yet. In this article, we aim to discuss the clinical applications and future directions of blood flow assessment in aortic surgery. We then provide our unique perspective on the technique's translational impact on the surgical management of aortic disease.

Methods: Articles from the PubMed database and Google Scholar regarding blood flow assessment in aortic surgery were reviewed. For the initial search, articles published between 2013 and 2023 were prioritized, including original articles, clinical trials, case reports, and reviews. Following the initial search, additional articles were considered based on manual searches of the references from the retrieved literature.

Key Content and Findings: In aortic root pathology and ascending aortic aneurysms, blood flow assessment can elucidate postoperative hemodynamic changes after surgical reconfiguration of the aortic valve complex or ascending aorta. In cases of aortic dissection, analysis of blood flow can predict future aortic dilatation. For complicated congenital aortic anomalies, surgeons may use preoperative imaging to perform "virtual surgery", in which blood flow assessment can predict postoperative hemodynamics for different surgical reconstructions and assist in procedural planning even before entering the operating room.

Conclusions: Blood flow assessment and computational modeling can evaluate hemodynamics and flow patterns by visualizing blood flow and calculating biomechanical forces in patients with aortic disease. We anticipate that blood flow assessment will become an essential tool in the treatment planning and understanding of the progression of aortic disease.

Keywords: Blood flow assessment; four-dimensional flow magnetic resonance imaging (4D flow MRI); computational fluid dynamics (CFDs); vector flow mapping (VFM); aortic surgery

Submitted Nov 22, 2023. Accepted for publication Feb 23, 2024. Published online Apr 18, 2024.
doi: 10.21037/jtd-23-1795
View this article at: https://dx.doi.org/10.21037/jtd-23-1795

Introduction

Aortic aneurysms and dissection are believed to be, at least in part, induced by alterations in blood flow dynamics (1). Rapid advances in imaging technology have allowed for innovations in aortic and cardiovascular imaging (2). The blood flow inside the aortic lumen can be visualized and analyzed by processing the data obtained through traditional modalities such as computed tomography (CT) or echocardiography in order to reveal novel hemodynamic information (3). Furthermore, blood flow assessment can provide information on the mechanical stress imparted by flowing blood on the aortic intima and ventricular endocardium (3,4), and so can provide unique clinical insights into the pathophysiology of aortic and cardiovascular disease (5,6). In this article, we summarize recent publications on blood flow assessment and discuss potential clinical applications and the future outlook of this novel approach. We then provide our unique perspective on the technique's translational impact on the surgical management of aortic disease. We present this article in accordance with the Narrative Review reporting checklist (available at https://jtd.amegroups.com/article/view/10.21037/jtd-23-1795/rc).

Methods

Searches of the PubMed and Google Scholar databases were conducted to identify published literature on the blood flow assessment for cardiovascular disease using the following terms: "blood flow assessment", "4D flow MRI", "computational fluid dynamics", "vector flow mapping", "echocardiography flow visualization", "aortic dissection", "aortic aneurysm", "aortic root surgery", "aortic surgery", "congenital aortic anomaly" and "aortic disease". For the initial search, articles published between 2013 and 2023 were prioritized. Original articles, clinical trials, case reports, and reviews were also included. Following the initial search, additional articles were considered based on manual searches of the references from the retrieved literature. The search strategy is summarized in *Table 1*.

How does blood flow assessment work?

Blood flow assessment includes two different technologies: first, image-based flow measurement and visualization, such as echocardiographic flow visualization or four-dimensional flow magnetic resonance imaging (4D flow MRI); and second, computer-based flow simulation using computational fluid dynamic (CFD) analysis (5,6). Below we will provide an overview of each of these techniques and discuss their applications to aortic disease.

Echocardiographic flow visualization

Several studies have reported on blood flow assessment with echocardiography (7-18). Particle imaging velocimetry (PIV), which uses tracer particles to measure the velocities of fluids, was found to quantify flow patterns *in vitro* accurately and precisely. Kim *et al.* first described its use in ultrasound imaging (7). Subsequently, echocardiographic PIV was utilized to evaluate blood flow patterns in patients with cardiovascular disease (8-11). However, Prinz *et al.* revealed that velocity estimation is accurate only up to a magnitude of 42 cm/s; at higher velocities, the accuracy depends on the acquisition parameters, such as the frame rate (12). Another method, echocardiographic vector flow mapping (VFM), utilizes the color Doppler mode to measure blood flow and assess flow dynamics in cardiovascular disease applications (13-18) (*Figure 1*). In VFM, the ultrasound data is processed using cross-correlation analysis, a complex mathematical process that compares the signals obtained from different ultrasound beams to determine the velocity of the blood flow in each direction. The data obtained from VFM can be used to detect and quantify abnormalities in blood flow, such as characterizing recirculation zones and turbulence immediately post stenosis (13-15). VFM is has been validated in experimental models, and like echocardiography, is non-invasive, easy to use, and available at the point of care (16). However, its use is significantly limited in patients who have complex 3-dimensional (3D) flow patterns (6), and its effectiveness is highly dependent on operator skill and variation in patient's anatomy (e.g.,

Table 1 The search strategy summary

Items	Specification
Date of search	March 1, 2023–August 31, 2023
Databases and other sources searched	PubMed, Google Scholar
Search terms used	"blood flow assessment", "4D flow MRI", "computational fluid dynamics", "vector flow mapping", "echocardiography flow visualization", "aortic dissection", "aortic aneurysm", "aortic root surgery", "aortic surgery", "congenital aortic anomaly" and "aortic disease"
Timeframe	2013–2023
Inclusion and exclusion criteria	Inclusion: original articles, clinical trials, case reports, and reviews were also included. Following the initial search, additional articles were considered based on manual searches of the references from the retrieved literature
	Exclusion: non-English articles were excluded
Selection process	Y.H. conducted the initial literature search. All authors conducted additional literature searches, reviewed the papers, and contributed to the final selection of paper

4D flow MRI, four-dimensional flow magnetic resonance imaging.

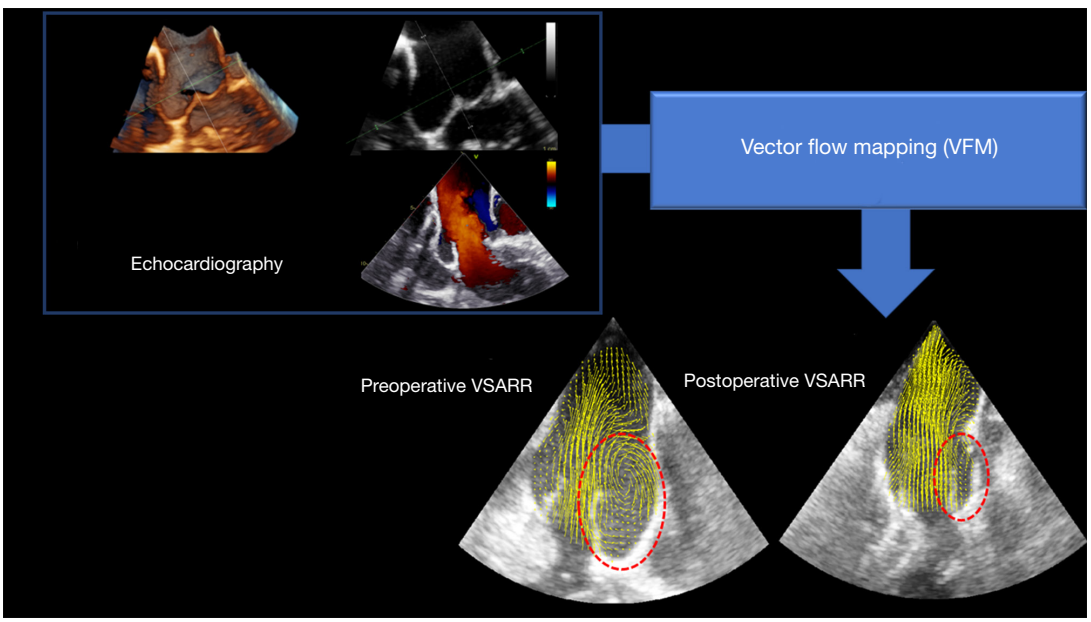

Figure 1 Echocardiographic VFM. VFM technology can visualize blood flow patterns using echocardiographic data. Here, flow patterns are shown before and after VSARR. A large vortex in the aneurysmal aortic root (highlighted in red) was identified on preoperative imaging and was resolved after surgical repair. Figure adapted with permission from Hayashi *et al.* (18). VFM, vector flow mapping; VSARR, valve-sparing aortic root replacement.

body habitus, chest deformity, lung disease, etc.).

4D flow MRI

4D flow MRI is another flow imaging modality based on direct *in vivo* flow measurements. This non-invasive method enables blood flow pattern visualization and quantification of regional blood flow and velocity in all 3 spatial directions resolved relative to the 3 dimensions of space and dimension of time along the cardiac cycle (3D + time = 4D) (19). 4D

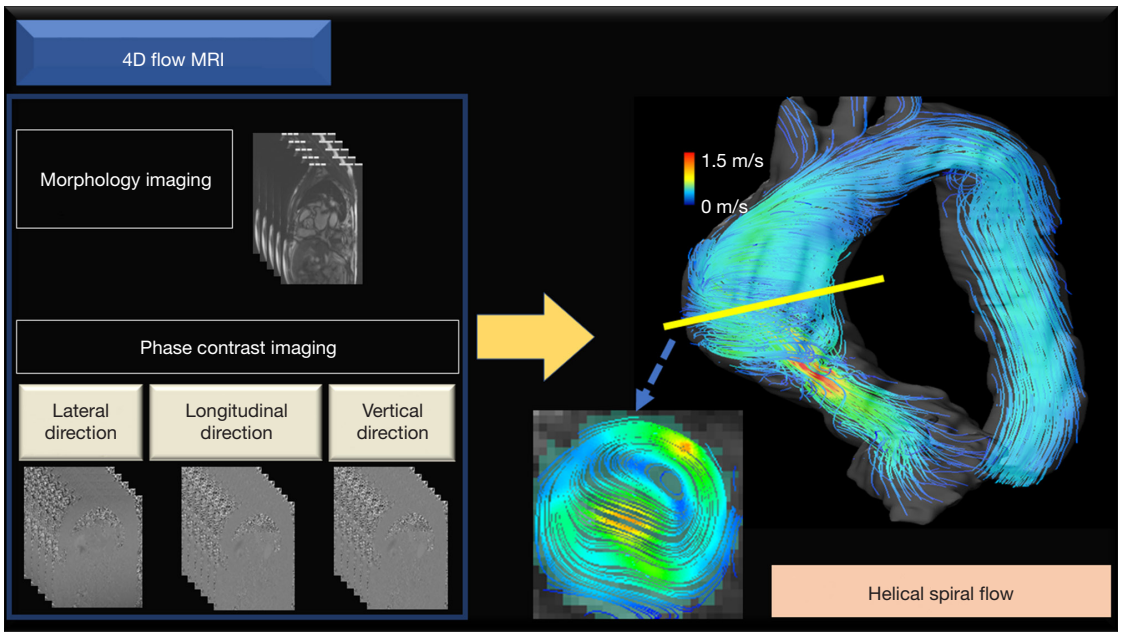

Figure 2 4D flow MRI-based blood flow assessment. 4D flow MRI can provide hemodynamic information using anatomical and phase-contrast imaging sequences. Transvalvular blood flow is shown here after surgical aortic valve replacement with a porcine valve. A helical spiral flow was observed in the ascending aorta during the holosystolic phase. Figure adapted with permission from Hohri *et al.* (22). 4D flow MRI, four-dimensional flow magnetic resonance imaging.

flow MRI can visualize the blood flow inside the vascular lumen by combining cine mode MRI, which captures the structure and motion of the heart during a cardiac cycle, and 3D-phase contrast imaging, which measures the blood flow velocity in every direction. By combining these methods, 4D flow MRI can extract a 3D velocity vector distribution and the motion of the blood flow in a blood vessel or a heart chamber throughout the cardiac cycle. It is currently the only method that can measure 3D blood flow with the vector component *in vivo*, and as such is a powerful tool in the evaluation of hemodynamics in cardiac disease. 4D flow MRI can even comprehensively capture cardiac structure and hemodynamic function in patients with complex anatomy (6,20). Recently, several commercial tools utilizing this imaging process have become available, leading to an increase in publications and clinical applications regarding 4D flow MRI (6). Although 4D flow MRI has several limitations, such as limited spatial and temporal resolution and aliasing errors, its clinical applications in cardiac disease have been published with acceptable reproducibility (21,22). For example, our group has reported on the difference in transvalvular flow between porcine and bovine pericardial bioprosthetic valves after aortic valve (AV) replacement (22) (*Figure 2*). A helical spiral flow, which is a flow with rotation around an axis while moving forward (23,24), was observed in the ascending aorta during the holosystolic phase. In contrast, a straight transvalvular aortic flow was observed in a bovine pericardial valve in the early systolic phase. Two large vortical flows, which are rotating or swirling flows with streamlines or pathlines that tend to curl back on themselves (23,24), occurred on both sides of the greater and lesser curvature of the ascending aorta after the mid-systolic period.

CFD modeling and analysis

Blood flow assessment using CFD has powerful applications in the predictive modeling of cardiovascular disease progression. CFD analysis involves solving a system of equations governing the blood flow derived from the first principles, including mass and momentum conservation, using complex numerical methods on geometries built from cardiovascular images and employing physiological flows or pressures as boundary conditions (6) (*Figure 3*). It is, however, important to distinguish that CFD analysis 'simulates' the flow based on the underlying assumptions and

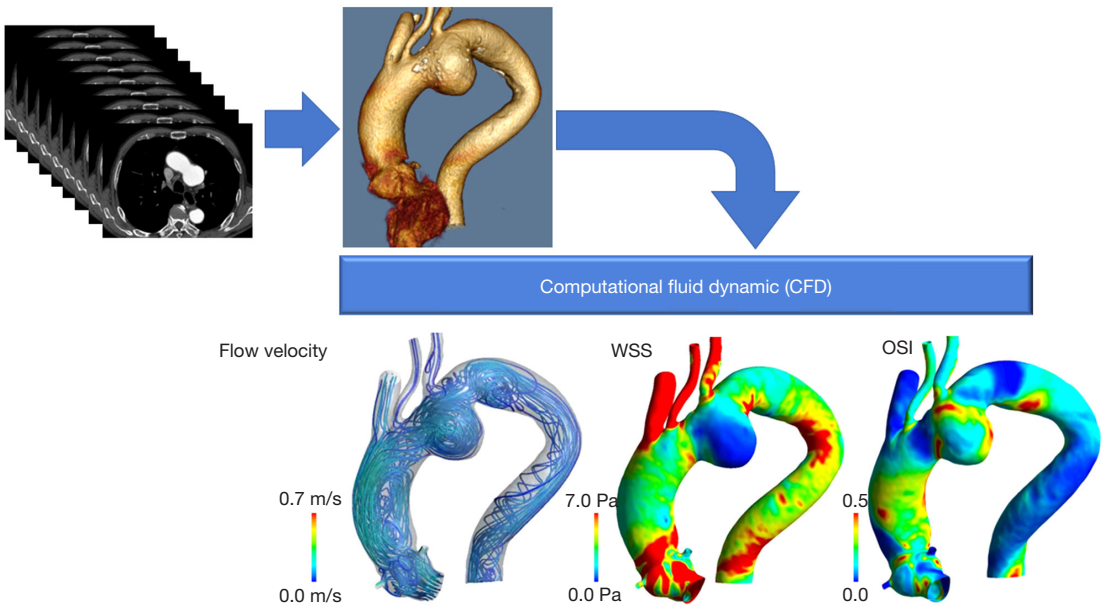

Figure 3 CFD analysis using CT imaging. Complex blood flow patterns can be simulated using CFD analysis on 3-dimensional patient-specific models constructed from CT imaging. CFD analysis can provide distributions of flow velocity, pressure gradients, WSS, or OSI. CFD, computational fluid dynamic; WSS, wall shear stress; OSI, oscillatory shear index; CT, computed tomography.

boundary conditions, and is sensitive to several parameters, including the type of numerical discretization, convergence, mesh resolution, etc., instead of providing the actual blood velocity measurements. Nevertheless, the strengths of CFD analysis are its ability to perform predictive modeling, evaluate alternative surgical designs toward surgical planning, design medical devices, and assess conditions that are otherwise challenging to evaluate using conventional image-based measurements, such as exercise intolerance (25-27). Furthermore, a notable advantage of CFD analysis is that it can be performed retrospectively on images that have already been captured, making its implementation and clinical utility more versatile as it does not require additional imaging or tests. However, the methods employed in the CFD analysis must be thoroughly validated using *in vivo* and *in vitro* data before successful adoption in the clinical setting because CFD analysis is calculated from assumed parameters (28). Another critical bottleneck of CFD analysis toward clinical adoption is the computational cost and the time-intensive workflow in patient-specific analysis. Therefore, CFD analysis may be best utilized when there is sufficient time before the operation. Machine learning techniques may potentially be utilized to accelerate the workflow and enhance objectivity (29).

How is blood flow assessment applied clinically?

Blood flow assessment can be clinically useful since it allows for visualization of blood flow and evaluation of blood flow patterns as well as quantitative evaluation of the dynamic properties of blood flow. In general, blood flow assessment enables the measurement of three clinically relevant parameters: flow energy loss (EL), wall shear stress (WSS), and oscillatory shear index (OSI).

EL refers to the viscous dissipation of kinetic energy. It is calculated as below:

$$\mathrm{EL}\,(\mathrm{mW}) = \int \mu \sum_{i,j} \left(\frac{\partial u_j}{\partial x_i} + \frac{\partial u_i}{\partial x_j} \right)^2 dv \qquad [1]$$

where μ is the coefficient of blood viscosity, μ is the velocity vector component, and i and j are coordinates on the Cartesian coordinate system (21,22).

In cardiovascular disease, it describes the incremental change in blood flow velocity distribution as blood moves through the heart and vasculature and so is used as a parameter of cardiac workload, with high EL signifying excessive work on the ventricular chamber (5,6,22) (*Figure 4*). This concept of kinetic energy dissipation has been emphasized the assessment of hemodynamic severity of aortic stenosis (AS) (30). It is well known that there can

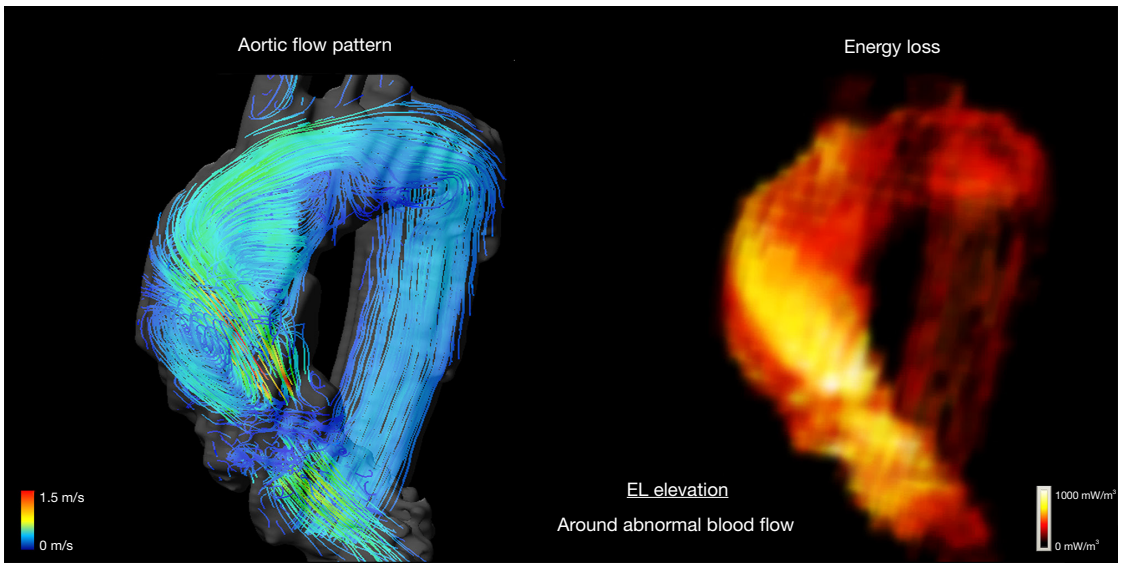

Figure 4 Flow EL. EL is defined as the loss of kinetic energy flow due to viscous dissipation enhanced by altered blood flow in a diseased aorta, which may increase cardiac workload. Transvalvular blood flow is shown here after surgical aortic valve replacement with a bovine pericardial valve. A straight transvalvular aortic jet was observed in the early systolic phase, and two large vortices were observed on both sides of the greater and lesser curvatures of the ascending aorta post-mid-systole. EL is increased around these complex flow distributions in the ascending aorta. Figure adapted with permission from Hohri *et al.* (22). EL, energy loss.

be discrepancies in the assessment of hemodynamic severity in AS between echocardiography and catheterization because echocardiography does not account for the extent of pressure recovery that occur downstream of the stenosis by dissipation of energy (31). When significant pressure recovery occurs, the echocardiography-measured transvalve gradient can markedly exceed catheterization-measured gradient (32). This irreversible gradient, which is calculated taking into account pressure recovery, is currently best estimated by catheterization; however, this is invasive which limits its routine use. In contrast, 4D flow MRI permits noninvasive estimation of EL with flow visualization. Previously, several studies reported that EL measured by 4D flow MRI correlated strongly with irreversible pressure gradient (33,34). These studies concluded that EL can provide complementary information to well-established method, helping assess AS severity in patients whose diagnosis is challenging due to subtle examination findings.

WSS is the shear force on the vessel wall caused by blood flow and is calculated from the flow velocity profile within the vessel lumen (6,35) (*Figure 5*). Previously, the normal range of WSS was reported between 1 and 7 Pa in the coronary artery. The WSS is reported to be closely related to endothelial degeneration of the vessel wall in atherosclerotic disease (36,37). Interestingly, both low and high WSS have been reported as risk factors for aneurysm formation (37,38). Salmasi *et al.* found that elevated WSS was predictive of reduced wall thickness, elastin and smooth muscle cell count, indicative of reduced vessel compliance (38), whereas long-term exposure to low WSS on the aneurysm wall was reported to increase intercellular permeability and induces severe elasticity degradation in the aneurysm (39). Moreover, a high WSS on the coronary arterial wall promotes plaque rupture, whereas a low WSS accelerates plaque progression and facilitates arterial remodeling through apoptosis and proliferation (40-42). On valvular leaflets, an elevated WSS activates the valvular endothelium on the fibrosa via bone morphogenetic protein-4- and transforming growth factor-beta1-dependent pathways, promoting the fibrosis and calcification of valves that eventually result in progressive stenosis (43).

OSI measures the degree of fluctuation in shear stress orientation over a cardiac cycle (5,35) (*Figure 5*). An OSI value close to 0.5 indicates that WSS experienced a 180° change in its orientation during the cycle, while an OSI value of 0 indicates that the WSS vector did not change its direction throughout the cycle. It is defined as follows:

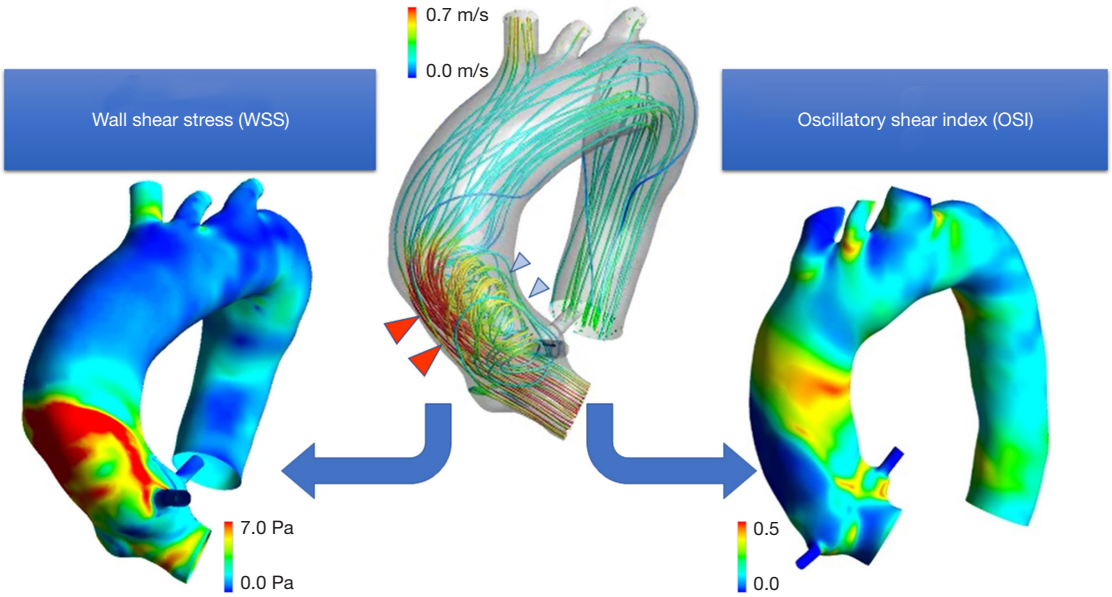

Figure 5 WSS and OSI. CFD analysis using pre-onset CT imaging in a patient with acute type A aortic dissection. WSS, or the stress induced on the endothelial wall by the near-wall blood flow, is increased in the posterolateral segment of the proximal ascending aorta (red arrows) due to the impingement of the transvalvular jet. OSI measures the three-dimensional fluctuation of the WSS vector during a cardiac cycle. OSI is increased around the location of vortex flow on the side of the lesser curvature of ascending aorta (blue arrows). Figure adapted with permission from Hohri *et al.* (35). WSS, wall shear stress; OSI, oscillatory shear index; CFD, computational fluid dynamic; CT, computed tomography.

$$OSI = \frac{1}{2}\left(1 - \frac{\left|\int_0^T \overrightarrow{WSS}dt\right|}{\int_0^T \left|\overrightarrow{WSS}\right|dt}\right) \quad [2]$$

Fluid shear stress, such as OSI, has vital implications on endothelial mechanotransduction (44). Hwang *et al.* reported that oscillatory shear increases reactive oxygen production in endothelial cells to a greater extent than laminar shear. The increased reactive oxygen production in endothelial cells due to high OSI results in fibrous tissue regeneration following endothelial injury (5,45). Therefore, high OSI can predict the occurrence of aortic dissection and AV leaflet degeneration (35,46). Thus, mechanical stress parameters measured by blood flow assessment can be used as diagnostic parameters in the clinical management of cardiovascular disease.

Clinical application of blood flow assessment in aortic disease

AV and aortic root

More than a quarter century ago, a vortex (or recirculatory flow) was demonstrated in the Sinus of Valsalva (SOV) using 4D flow MRI (47); the clinical relevance of this vortical flow in aortic root surgery has since been explored (48). Keller *et al.* observed that, in patients with root aneurysms and altered aortic flow dynamics, helical and vortical flows in the ascending aorta were significantly improved to physiological levels after aortic root replacement (49). Oechtering *et al.* found that the flow pattern within a Valsalva-shaped graft after valve-sparing aortic root repair (VSARR) with an anatomically-shaped sinus prosthesis was closely related to that in healthy volunteers (50). Subsequently, aortic root surgery reduced abnormal blood flow within the aortic lumen and mechanical stress on the aortic wall (51). Moreover, Semaan *et al.* demonstrated that the parameters of flow eccentricity normalized after VSARR for both tricuspid and bicuspid aortic valves (BAVs); however, when compared to preoperative values, they observed increased peak systolic velocities and acceleration in the aortic root, ascending aorta, and descending aorta, particularly in patients with BAVs (52). Collins *et al.* found that, compared to the Bentall procedure with a bioprosthetic valve, a VSARR resulted in more physiological hemodynamics with

reduced forward flow impingement on the aortic wall of the ascending aorta (53). Additional follow-up is warranted to investigate the influence of these findings on vascular physiology and patient outcomes (52).

VFM is also helpful in evaluating hemodynamics in patients with aortic root aneurysms. Our group reported a unique approach to investigating the influence of aortic root geometry on AV leaflets, using epi-aortic echocardiography to measure the mechanical stress on the AV leaflet (17). We also visualized vortex flow in aortic root aneurysms, which were contributing to the high WSS and OSI on AV leaflets; these abnormal mechanical stresses decreased significantly after VSARR. Moreover, we revealed that an aneurysmal aortic root exposes the AV leaflets to abnormal fluid dynamics by correlating the size of the SOV with the systolic WSS and OSI (18).

Ascending aorta and aortic arch

4D flow MRI has contributed to our understanding of the association between BAV and ascending aortic aneurysms (54-57). Eccentric flow, which is an abnormal transvalvular flow caused by bicuspid valvular morphology, is thought to be an important contributor to the aortopathy in patients with BAV (58,59). Lorenz *et al.* showed that, compared to the normal helical flow in the ascending aorta and arch observed in patients with tricuspid AV, patients with BAV had a significantly higher absolute peak helicity throughout the thoracic aorta (54). The eccentric flow during systole in the ascending aorta was found to have a profound and asymmetrically elevated WSS, a known risk factor for triggering ascending aortic aneurysms (56,57). These 4D flow MRI studies suggest that abnormal eccentric aortic blood flow contributes to the development and growth of ascending aortic aneurysms. Previously, Numata *et al.* investigated the difference in systemic and cerebral perfusion flow patterns between subclavian artery cannulation and ascending aorta cannulation during ascending aorta or arch replacement using CFD analysis; they reported that right subclavian artery cannulation produced a protective effect on the brain, especially on the right side (60). Thus, blood flow assessment may play an important role on the surgical management of aortic disease.

Aortic dissection

Several previous studies have reported on the utility of blood flow assessment in aortic dissection (35,61-68). Our group performed CFD analysis on pre-onset CT images of patients with acute type A aortic dissection (AAAD) to elucidate the mechanism of primary entry occurrence in the AAAD (35). We found that shear stress fluctuations were closely associated with the future occurrence of AAAD (*Figure 6*). Bäumler *et al.* proved that mobility of the dissected flap substantially influences local hemodynamics and therefore needs to be accounted for in patient-specific simulations of aortic dissection (61). Furthermore, CFD analysis can assist in predicting aortic dilation on follow-up of patients with aortic dissection (62,63). Shang *et al.* visualized blood flow using CFD analysis and found that greater flow diversion to the false lumen and increased WSS on the aortic wall were associated with rapid aortic growth (63). Similarly, increased WSS was associated with retrograde AAAD in patients with acute type B aortic dissection (TBAD) (64).

There is growing interest in the distal aorta with residual dissection after repair of the proximal aorta for AAAD (69,70). Some studies have investigated postoperative remodeling of the descending aorta using CFD analysis (65-67). Zhu *et al.* reported that the pressure difference between the true and false lumens could predict progressive residual native aortic dilatation after primary surgery in patients with AAAD. They found that a pressure difference >5 mmHg may be related to unstable aortic growth (67). Moreover, Liu *et al.* investigated the differences in flow velocity and wall pressure (the force on the vessel wall caused by blood flow) between patients with two and multiple entry tears in patients with TBAD. They showed that TBAD with two entry tears squeezes the true lumen and expands the false lumen with higher wall pressure, resulting in a new entry tear and deterioration into multiple entry-TBAD. Therefore, they concluded that the closure of the proximal entry tear was deemed ideal solution for TBAD with two entry tears (68). Thus, CFD analysis plays an important role as a predictor of the progression of aortic disease leading to dissection.

Congenital aortic anomalies

The use of blood flow analysis in cases of congenital aortic anomalies has shown promising results. Previous studies have evaluated the hemodynamics of aortic coarctation using 4D flow MRI and CFD analysis (71,72). Rengier *et al.* used 4D flow MRI to non-invasively compare the alteration of pressure distribution in patients with and without aortic

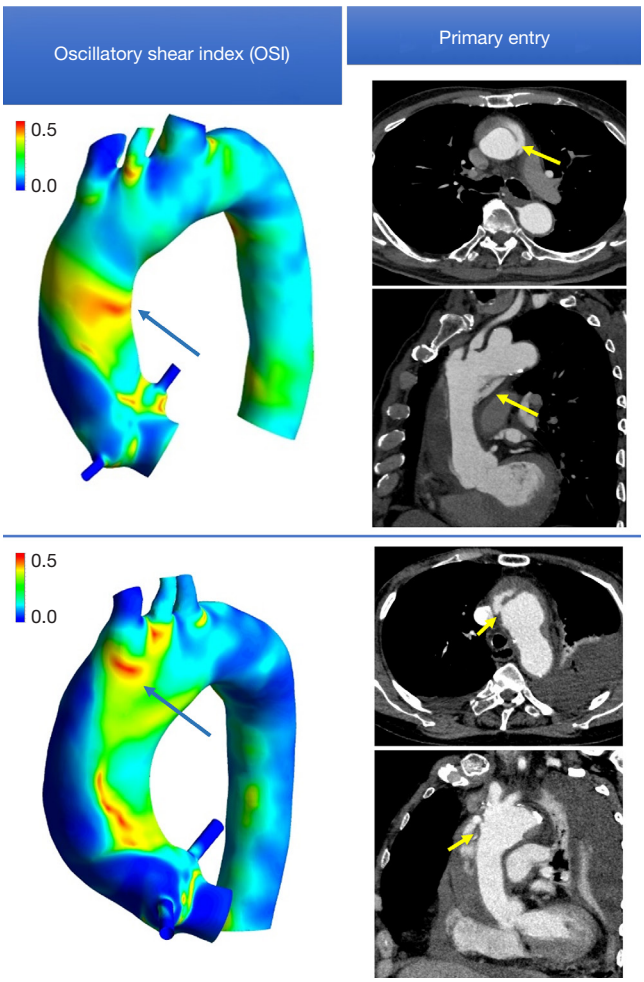

Figure 6 Result of CFD analysis using retrospective pre-onset CT imaging in two patients with AAAD. A concentrated high OSI area was observed around the recirculatory flow (blue arrows). These hot spots with high OSI are near the primary entry site of an impending AAAD (yellow arrows). Figure adapted with permission from Hohri *et al.* (35). OSI, oscillatory shear index; CFD, computational fluid dynamic; CT, computed tomography; AAAD, acute type A aortic dissection.

coarctation repair (71). Lantz *et al.* evaluated mechanical stresses in a patient with coarctation before and after repair. They concluded that these forces may be useful diagnostic indicators for assessing the success of intervention (72). Lastly, our group used CFD analysis to guide clinical treatment in patients with double aortic arch (73). In this complex physiology, various anatomical features such as the shape and the angle of the aortic bifurcation and the aortic diameter make it challenging to identify the dominant arch; CFD analysis was used to evaluate the flow volumes into each aortic arch and thus guide appropriate treatment plan (72).

Current limitations of blood flow assessment

Blood flow assessment has several limitations. First, although it can evaluate mechanical stress parameters, including EL, WSS, and OSI, there are no unified reference or cut-off values because these parameters depend on mean blood volume, flow velocity, its variation near the wall, vessel diameter, and blood viscosity, resulting in wide variation among vessels and the ventricular chambers (74). For example, EL was different between left and right ventricles even in healthy volunteers' case (75). Thus, a statistical baseline has yet to be established due to limited data. 4D flow MRI and echocardiographic VFM have limited temporal and spatial resolutions, and accelerated jet flow may cause aliasing artifacts, although they can be rectified during post-processing. However, since 4D flow MRI and echocardiographic VFM can visualize actual blood flow, these modalities are advantageous in assessing complex hemodynamics in the ascending aorta or the aortic root. The aortic valvular complex significantly influences the hemodynamics in the aortic root and ascending aorta. In CFD analysis, fluid-structure interactions are required to evaluate the influence of aortic valvular motion. Although some studies have reported limited use of CFD across the AV (76,77), it has not yet been clinically applied owing to the computational cost and complexity. Moreover, in CFD analysis, the aortic wall is typically assumed to be rigid due to the difficulty in estimating the tissue properties of individual patients. Further, while standalone CFD analysis has been instrumental in revealing novel hemodynamic insights in aortic disease, a clinically meaningful impact can only be realized by applying CFD analysis to large patient cohorts.

Future perspective of blood flow assessment in aortic surgery

"Virtual surgery"

When combined with 3D computer graphics, CFD analysis can enable aortic surgeons to perform "virtual surgery" (6,78). Virtual surgery predicts postoperative blood flow, which can supplement preoperative surgical planning based on an individual's hemodynamics in aortic

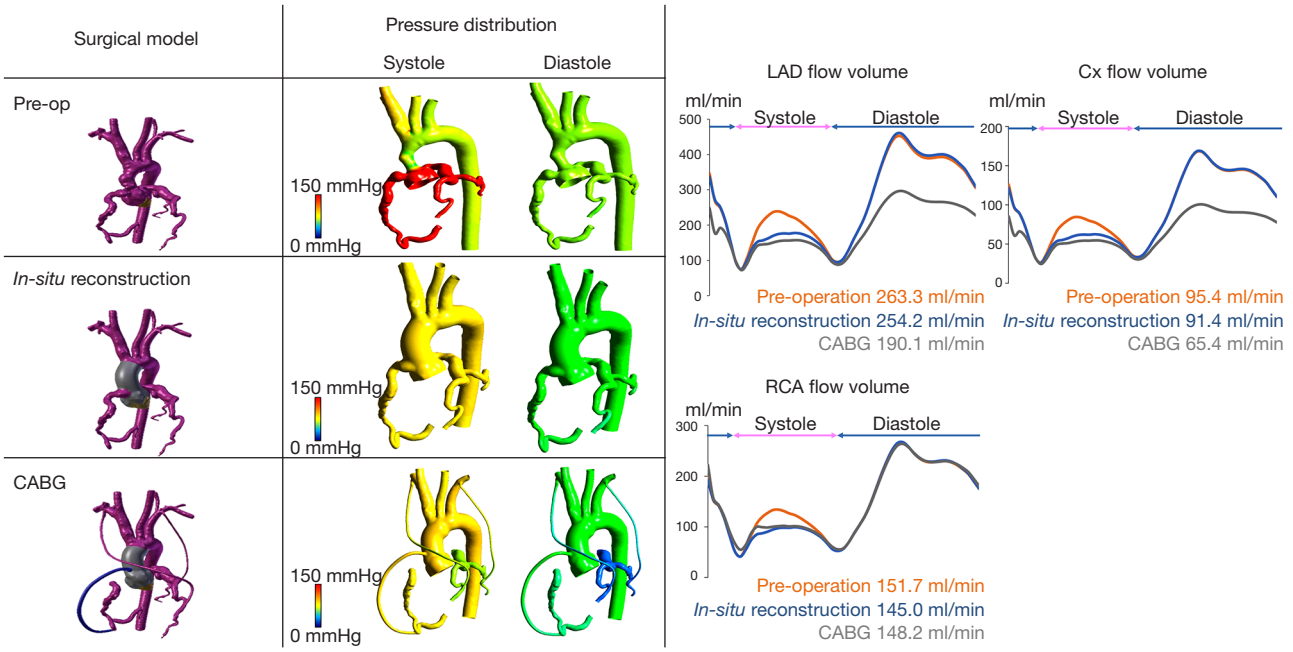

Figure 7 Virtual surgery to guide preoperative planning in aortic root surgery. A Pre-op and two computer-based virtual postoperative models were created: (I) *in situ* coronary reconstruction with Carrel patch technique for root replacement; (II) CABG procedure connecting the bilateral ITA to the LAD and Cx, and the saphenous vein graft connecting the ascending aorta to the RCA in addition to root replacement. CFD analysis showed lower coronary pressure and a shortage of blood supply to the left coronary arteries in the CABG model despite using the bilateral ITA. In contrast, in the *in-situ* revascularization model, the systolic coronary blood flow decreased due to the reduction in the Valsalva pressure but with sufficiently increased coronary flow during diastole. Figure adapted with permission from Hohri *et al.* (80). Pre-op, preoperative model; CABG, coronary artery bypass grafting; LAD, left anterior descending artery; Cx, circumflex branches; RCA, right coronary artery; ITA, internal thoracic artery; CFD, computational fluid dynamic.

disease. In this method, the patient-specific geometry acquired from preoperative CT imaging is morphed into a predicted postoperative anatomy, and blood flow is computed following the simulated repair (6). For example, Fujisue *et al.* utilized virtual surgery to guide preoperative planning in patients with aortic coarctation. They compared the postoperative hemodynamics between three surgical approaches: ascending-abdominal aorta bypass, descending-descending aorta bypass, and descending aorta replacement; their calculations helped guide the approach ultimately pursued in the operating room (79). We used this technology to decide whether to pursue concomitant coronary revascularization during aortic root replacement for a patient with supravalvular aortic root stenosis. After comparing postoperative coronary flow volume following a Bentall procedure with and without concomitant coronary artery bypass grafting (CABG), a preoperative decision to perform an isolated Bentall was made (*Figure* 7) (80). Virtual surgery with CFD analysis can help determine the optimal surgical procedure personalized to an individual during preoperative planning.

Conclusions

Blood flow assessment has been increasingly applied to the clinical management of aortic disease. It can enable the evaluation of hemodynamics by visualizing blood flow and estimating the degree of mechanical stress on the aortic wall or valve leaflets. Furthermore, blood flow assessment can predict postoperative hemodynamics and future aortic degeneration. In cases with complicated anatomy, such as in congenital aortic disease, it can be valuable in understanding the hemodynamics of individual patients. Moreover, "virtual surgery" can help determine the optimal surgical strategy for patients with complex anatomy. Thus, blood flow assessment has the capacity to become an essential tool for aortic experts.

Acknowledgments

Funding: None.

Footnote

Reporting Checklist: The authors have completed the Narrative Review reporting checklist. Available at https://jtd.amegroups.com/article/view/10.21037/jtd-23-1795/rc

Peer Review File: Available at https://jtd.amegroups.com/article/view/10.21037/jtd-23-1795/prf

Conflicts of Interest: All authors have completed the ICMJE uniform disclosure form (available at https://jtd.amegroups.com/article/view/10.21037/jtd-23-1795/coif). H.T. serves as an unpaid editorial board member of *Journal of Thoracic Disease* from October 2022 to January 2025. H.T. receives a research grant from the Rudin Foundation. The other authors have no conflicts of interest to declare.

Ethical Statement: The authors are accountable for all aspects of the work in ensuring that questions related to the accuracy or integrity of any part of the work are appropriately investigated and resolved.

References

1. Gao J, Cao H, Hu G, et al. The mechanism and therapy of aortic aneurysms. Signal Transduct Target Ther 2023;8:55.
2. Di Carli MF, Geva T, Davidoff R. The Future of Cardiovascular Imaging. Circulation 2016;133:2640-61.
3. Whitlock MC, Hundley WG. Noninvasive Imaging of Flow and Vascular Function in Disease of the Aorta. JACC Cardiovasc Imaging 2015;8:1094-106.
4. Stoll VM, Hess AT, Rodgers CT, et al. Left Ventricular Flow Analysis. Circ Cardiovasc Imaging 2019;12:e008130.
5. Itatani K. Advances in Hemodynamics Research. Hauppauge: Nova Science Publishers, 2015.
6. Itatani K, Miyazaki S, Furusawa T, et al. New imaging tools in cardiovascular medicine: computational fluid dynamics and 4D flow MRI. Gen Thorac Cardiovasc Surg 2017;65:611-21.
7. Kim HB, Hertzberg JR, Shandas R. Development and validation of echo PIV. Exp Fluids 2004;36:455-62.
8. Faludi R, Szulik M, D'hooge J, et al. Left ventricular flow patterns in healthy subjects and patients with prosthetic mitral valves: an in vivo study using echocardiographic particle image velocimetry. J Thorac Cardiovasc Surg 2010;139:1501-10.
9. Sengupta PP, Pedrizetti G, Narula J. Multiplanar visualization of blood flow using echocardiographic particle imaging velocimetry. JACC Cardiovasc Imaging 2012;5:566-9.
10. Gürel E, Prinz C, Van Casteren L, et al. The Impact of Function-Flow Interaction on Left Ventricular Efficiency in Patients with Conduction Abnormalities: A Particle Image Velocimetry and Tissue Doppler Study. J Am Soc Echocardiogr 2016;29:431-40.
11. Agati L, Cimino S, Tonti G, et al. Quantitative analysis of intraventricular blood flow dynamics by echocardiographic particle image velocimetry in patients with acute myocardial infarction at different stages of left ventricular dysfunction. Eur Heart J Cardiovasc Imaging 2014;15:1203-12.
12. Prinz C, Faludi R, Walker A, et al. Can echocardiographic particle image velocimetry correctly detect motion patterns as they occur in blood inside heart chambers? A validation study using moving phantoms. Cardiovasc Ultrasound 2012;10:24.
13. Nakashima K, Itatani K, Kitamura T, et al. Energy dynamics of the intraventricular vortex after mitral valve surgery. Heart Vessels 2017;32:1123-9.
14. Akiyama K, Nakamura N, Itatani K, et al. Flow-dynamics assessment of mitral-valve surgery by intraoperative vector flow mapping. Interact Cardiovasc Thorac Surg 2017;24:869-75.
15. Akiyama K, Itatani K, Naito Y, et al. Vector Flow Mapping and Impaired Left Ventricular Flow After the Alfieri Stitch. J Cardiothorac Vasc Anesth 2017;31:211-4.
16. Uejima T, Koike A, Sawada H, et al. A new echocardiographic method for identifying vortex flow in the left ventricle: numerical validation. Ultrasound Med Biol 2010;36:772-88.
17. Hayashi H, Akiyama K, Itatani K, et al. A novel in vivo assessment of fluid dynamics on aortic valve leaflet

using epi-aortic echocardiogram. Echocardiography 2020;37:323-30.
18. Hayashi H, Itatani K, Akiyama K, et al. Influence of aneurysmal aortic root geometry on mechanical stress to the aortic valve leaflet. Eur Heart J Cardiovasc Imaging 2021;22:986-94.
19. Soulat G, McCarthy P, Markl M. 4D Flow with MRI. Annu Rev Biomed Eng 2020;22:103-26.
20. Itatani K, Sekine T, Yamagishi M, et al. Hemodynamic Parameters for Cardiovascular System in 4D Flow MRI: Mathematical Definition and Clinical Applications. Magn Reson Med Sci 2022;21:380-99.
21. Morichi H, Itatani K, Yamazaki S, et al. Influences of mitral annuloplasty on left ventricular flow dynamics assessed with 3-dimensional cine phase-contrast flow magnetic resonance imaging. J Thorac Cardiovasc Surg 2022;163:947-59.
22. Hohri Y, Itatani K, Numata S, et al. Blood flow energy loss: a predictor for the recovery of left ventricular function after bioprosthetic aortic valve replacement. Interact Cardiovasc Thorac Surg 2021;33:339-47.
23. Markl M, Kilner PJ, Ebbers T. Comprehensive 4D velocity mapping of the heart and great vessels by cardiovascular magnetic resonance. J Cardiovasc Magn Reson 2011;13:7.
24. von Spiczak J, Crelier G, Giese D, et al. Quantitative Analysis of Vortical Blood Flow in the Thoracic Aorta Using 4D Phase Contrast MRI. PLoS One 2015;10:e0139025.
25. Marsden AL, Bernstein AJ, Reddy VM, et al. Evaluation of a novel Y-shaped extracardiac Fontan baffle using computational fluid dynamics. J Thorac Cardiovasc Surg 2009;137:394-403.e2.
26. Marsden AL, Vignon-Clementel IE, Chan FP, et al. Effects of exercise and respiration on hemodynamic efficiency in CFD simulations of the total cavopulmonary connection. Ann Biomed Eng 2007;35:250-63.
27. Vahidkhah K, Barakat M, Abbasi M, et al. Valve thrombosis following transcatheter aortic valve replacement: significance of blood stasis on the leaflets. Eur J Cardiothorac Surg 2017;51:927-35.
28. Vedula V, Fortini S, Seo JH, et al. Computational modeling and validation of intraventricular flow in a simple model of the left ventricle. Theoretical and Computational Fluid Dynamics 2014;28:589-604.
29. Kong F, Shadden SC. Automating Model Generation for Image-Based Cardiac Flow Simulation. J Biomech Eng 2020;142:111011.
30. Pibarot P, Garcia D, Dumesnil JG. Energy loss index in aortic stenosis: from fluid mechanics concept to clinical application. Circulation 2013;127:1101-4.
31. Garcia D, Dumesnil JG, Durand LG, et al. Discrepancies between catheter and Doppler estimates of valve effective orifice area can be predicted from the pressure recovery phenomenon: practical implications with regard to quantification of aortic stenosis severity. J Am Coll Cardiol 2003;41:435-42.
32. Niederberger J, Schima H, Maurer G, et al. Importance of pressure recovery for the assessment of aortic stenosis by Doppler ultrasound. Role of aortic size, aortic valve area, and direction of the stenotic jet in vitro. Circulation 1996;94:1934-40.
33. Dyverfeldt P, Hope MD, Tseng EE, et al. Magnetic resonance measurement of turbulent kinetic energy for the estimation of irreversible pressure loss in aortic stenosis. JACC Cardiovasc Imaging 2013;6:64-71.
34. Binter C, Gotschy A, Sündermann SH, et al. Turbulent Kinetic Energy Assessed by Multipoint 4-Dimensional Flow Magnetic Resonance Imaging Provides Additional Information Relative to Echocardiography for the Determination of Aortic Stenosis Severity. Circ Cardiovasc Imaging 2017;10:e005486.
35. Hohri Y, Numata S, Itatani K, et al. Prediction for future occurrence of type A aortic dissection using computational fluid dynamics. Eur J Cardiothorac Surg 2021;60:384-91.
36. Cunningham KS, Gotlieb AI. The role of shear stress in the pathogenesis of atherosclerosis. Lab Invest 2005;85:9-23.
37. Stone PH, Saito S, Takahashi S, et al. Prediction of progression of coronary artery disease and clinical outcomes using vascular profiling of endothelial shear stress and arterial plaque characteristics: the PREDICTION Study. Circulation 2012;126:172-81.
38. Salmasi MY, Pirola S, Sasidharan S, et al. High Wall Shear Stress can Predict Wall Degradation in Ascending Aortic Aneurysms: An Integrated Biomechanics Study. Front Bioeng Biotechnol 2021;9:750656.
39. Mutlu O, Salman HE, Al-Thani H, et al. How does hemodynamics affect rupture tissue mechanics in abdominal aortic aneurysm: Focus on wall shear stress derived parameters, time-averaged wall shear stress, oscillatory shear index, endothelial cell activation potential, and relative residence time. Comput Biol Med 2023;154:106609.
40. Fukumoto Y, Hiro T, Fujii T, et al. Localized elevation of shear stress is related to coronary plaque rupture: a 3-dimensional intravascular ultrasound study with in-

vivo color mapping of shear stress distribution. J Am Coll Cardiol 2008;51:645-50.
41. Chatzizisis YS, Jonas M, Coskun AU, et al. Prediction of the localization of high-risk coronary atherosclerotic plaques on the basis of low endothelial shear stress: an intravascular ultrasound and histopathology natural history study. Circulation 2008;117:993-1002.
42. Doyle BJ, McGloughlin TM, Kavanagh EG, et al. From Detection to Rupture: A Serial Computational Fluid Dynamics Case Study of a Rapidly Expanding, Patient-Specific, Ruptured Abdominal Aortic Aneurysm. In: Doyle B, Miller K, Wittek A, et al. editors. Computational Biomechanics for Medicine. New York, NY, USA: Springer, 2014:53-68.
43. Wang W, Vootukuri S, Meyer A, et al. Association between shear stress and platelet-derived transforming growth factor-β1 release and activation in animal models of aortic valve stenosis. Arterioscler Thromb Vasc Biol 2014;34:1924-32.
44. Tzima E, Irani-Tehrani M, Kiosses WB, et al. A mechanosensory complex that mediates the endothelial cell response to fluid shear stress. Nature 2005;437:426-31.
45. Hwang J, Saha A, Boo YC, et al. Oscillatory shear stress stimulates endothelial production of O2- from p47phox-dependent NAD(P)H oxidases, leading to monocyte adhesion. J Biol Chem 2003;278:47291-8.
46. Mahler GJ, Frendl CM, Cao Q, et al. Effects of shear stress pattern and magnitude on mesenchymal transformation and invasion of aortic valve endothelial cells. Biotechnol Bioeng 2014;111:2326-37.
47. Kilner PJ, Yang GZ, Mohiaddin RH, et al. Helical and retrograde secondary flow patterns in the aortic arch studied by three-directional magnetic resonance velocity mapping. Circulation 1993;88:2235-47.
48. Markl M, Draney MT, Miller DC, et al. Time-resolved three-dimensional magnetic resonance velocity mapping of aortic flow in healthy volunteers and patients after valve-sparing aortic root replacement. J Thorac Cardiovasc Surg 2005;130:456-63.
49. Keller EJ, Malaisrie SC, Kruse J, et al. Reduction of aberrant aortic haemodynamics following aortic root replacement with a mechanical valved conduit. Interact Cardiovasc Thorac Surg 2016;23:416-23.
50. Oechtering TH, Hons CF, Sieren M, et al. Time-resolved 3-dimensional magnetic resonance phase contrast imaging (4D Flow MRI) analysis of hemodynamics in valve-sparing aortic root repair with an anatomically shaped sinus prosthesis. J Thorac Cardiovasc Surg 2016;152:418-427.e1.
51. Lenz A, Petersen J, Riedel C, et al. 4D flow cardiovascular magnetic resonance for monitoring of aortic valve repair in bicuspid aortic valve disease. J Cardiovasc Magn Reson 2020;22:29.
52. Semaan E, Markl M, Malaisrie SC, et al. Haemodynamic outcome at four-dimensional flow magnetic resonance imaging following valve-sparing aortic root replacement with tricuspid and bicuspid valve morphology. Eur J Cardiothorac Surg 2014;45:818-25.
53. Collins JD, Semaan E, Barker A, et al. Comparison of Hemodynamics After Aortic Root Replacement Using Valve-Sparing or Bioprosthetic Valved Conduit. Ann Thorac Surg 2015;100:1556-62.
54. Lorenz R, Bock J, Barker AJ, et al. 4D flow magnetic resonance imaging in bicuspid aortic valve disease demonstrates altered distribution of aortic blood flow helicity. Magn Reson Med 2014;71:1542-53.
55. Rodríguez-Palomares JF, Dux-Santoy L, Guala A, et al. Aortic flow patterns and wall shear stress maps by 4D-flow cardiovascular magnetic resonance in the assessment of aortic dilatation in bicuspid aortic valve disease. J Cardiovasc Magn Reson 2018;20:28.
56. van Ooij P, Potters WV, Collins J, et al. Characterization of abnormal wall shear stress using 4D flow MRI in human bicuspid aortopathy. Ann Biomed Eng 2015;43:1385-97.
57. Hope MD, Hope TA, Crook SE, et al. 4D flow CMR in assessment of valve-related ascending aortic disease. JACC Cardiovasc Imaging 2011;4:781-7.
58. Verma S, Siu SC. Aortic dilatation in patients with bicuspid aortic valve. N Engl J Med 2014;370:1920-9.
59. Minderhoud SCS, Roos-Hesselink JW, Chelu RG, et al. Wall shear stress angle is associated with aortic growth in bicuspid aortic valve patients. Eur Heart J Cardiovasc Imaging 2022;23:1680-9.
60. Numata S, Itatani K, Kawajiri H, et al. Computational fluid dynamics simulation of the right subclavian artery cannulation. J Thorac Cardiovasc Surg 2017;154:480-7.
61. Bäumler K, Vedula V, Sailer AM, et al. Fluid-structure interaction simulations of patient-specific aortic dissection. Biomech Model Mechanobiol 2020;19:1607-28.
62. Karmonik C, Partovi S, Müller-Eschner M, et al. Longitudinal computational fluid dynamics study of aneurysmal dilatation in a chronic DeBakey type III aortic dissection. J Vasc Surg 2012;56:260-3.e1.
63. Shang EK, Nathan DP, Fairman RM, et al. Use of computational fluid dynamics studies in predicting

aneurysmal degeneration of acute type B aortic dissections. J Vasc Surg 2015;62:279-84.
64. Osswald A, Karmonik C, Anderson JR, et al. Elevated Wall Shear Stress in Aortic Type B Dissection May Relate to Retrograde Aortic Type A Dissection: A Computational Fluid Dynamics Pilot Study. Eur J Vasc Endovasc Surg 2017;54:324-30.
65. Shad R, Kong S, Fong R, et al. Computational Fluid Dynamics Simulations to Predict False Lumen Enlargement After Surgical Repair of Type-A Aortic Dissection. Semin Thorac Cardiovasc Surg 2022;34:443-8.
66. Cheng SW, Lam ES, Fung GS, et al. A computational fluid dynamic study of stent graft remodeling after endovascular repair of thoracic aortic dissections. J Vasc Surg 2008;48:303-9; discusion 309-10.
67. Zhu Y, Xu XY, Rosendahl U, et al. Prediction of aortic dilatation in surgically repaired type A dissection: A longitudinal study using computational fluid dynamics. JTCVS Open 2022;9:11-27.
68. Liu H, Zhao G, Zhang GE, et al. Three-dimensional modelling and hemodynamic simulation of the closure of multiple entry tears in type B aortic dissection. Med Phys 2024;51:42-53.
69. Kimura N, Itoh S, Yuri K, et al. Reoperation for enlargement of the distal aorta after initial surgery for acute type A aortic dissection. J Thorac Cardiovasc Surg 2015;149:S91-8.e1.
70. Hohri Y, Yamasaki T, Matsuzaki Y, et al. Early and mid-term outcome of frozen elephant trunk using spinal cord protective perfusion strategy for acute type A aortic dissection. Gen Thorac Cardiovasc Surg 2020;68:1119-27.
71. Rengier F, Delles M, Eichhorn J, et al. Noninvasive 4D pressure difference mapping derived from 4D flow MRI in patients with repaired aortic coarctation: comparison with young healthy volunteers. Int J Cardiovasc Imaging 2015;31:823-30.
72. Lantz J, Ebbers T, Engvall J, et al. Numerical and experimental assessment of turbulent kinetic energy in an aortic coarctation. J Biomech 2013;46:1851-8.
73. Hohri Y, Numata S, Itatani K, et al. Determination of the dominant arch by computational fluid dynamics analysis using computed tomography images in double aortic arch. Int J Cardiovasc Imaging 2021;37:2573-5.
74. Papaioannou TG, Karatzis EN, Vavuranakis M, et al. Assessment of vascular wall shear stress and implications for atherosclerotic disease. Int J Cardiol 2006;113:12-8.
75. Nakaji K, Itatani K, Tamaki N, et al. Assessment of biventricular hemodynamics and energy dynamics using lumen-tracking 4D flow MRI without contrast medium. J Cardiol 2021;78:79-87.
76. Spühler JH, Jansson J, Jansson N, et al. 3D Fluid-Structure Interaction Simulation of Aortic Valves Using a Unified Continuum ALE FEM Model. Front Physiol 2018;9:363.
77. Halevi R, Hamdan A, Marom G, et al. Fluid-structure interaction modeling of calcific aortic valve disease using patient-specific three-dimensional calcification scans. Med Biol Eng Comput 2016;54:1683-94.
78. Miyaji K, Miyazaki S, Itatani K, et al. Novel surgical strategy for complicated pulmonary stenosis using haemodynamic analysis based on a virtual operation with numerical flow analysis. Interact Cardiovasc Thorac Surg 2019;28:775-82.
79. Fujisue J, Takayama Y, Tonoki S, et al. Utility of computational fluid dynamics for prediction of efficacy of the surgical interventions for aortic coarctation in adults. JTCVS Tech 2023;18:16-21.
80. Hohri Y, Itatani K, Yamazaki S, et al. Computerized virtual surgery based on computational fluid dynamics simulation for planning coronary revascularization with aortic root replacement in adult congenital heart disease: a case report. Gen Thorac Cardiovasc Surg 2021;69:722-6.

Cite this article as: Hohri Y, Chung MM, Kandula V, Kim I, Leb J, Hayashi H, Elmously A, O'Donnell TF, Patel V, Vedula V, Takayama H. Blood flow assessment technology in aortic surgery: a narrative review. J Thorac Dis 2024;16(4):2623-2636. doi: 10.21037/jtd-23-1795